Reovirus Activates a Caspase-Independent Cell Death Pathway

Angela K. Berger,[a] Pranav Danthi[b]

Department of Molecular and Cellular Biochemistry[a] and Department of Biology,[b] Indiana University, Bloomington, Indiana, USA

ABSTRACT **Virus-induced apoptosis is thought to be the primary mechanism of cell death following reovirus infection. Induction of cell death following reovirus infection is initiated by the incoming viral capsid proteins during cell entry and occurs via NF-κB-dependent activation of classical apoptotic pathways. Prototype reovirus strain T3D displays a higher cell-killing potential than strain T1L. To investigate how signaling pathways initiated by T3D and T1L differ, we methodically analyzed cell death pathways activated by these two viruses in L929 cells. We found that T3D activates NF-κB, initiator caspases, and effector caspases to a significantly greater extent than T1L. Surprisingly, blockade of NF-κB or caspases did not affect T3D-induced cell death. Cell death following T3D infection resulted in a reduction in cellular ATP levels and was sensitive to inhibition of the kinase activity of receptor interacting protein 1 (RIP1). Furthermore, membranes of T3D-infected cells were compromised. Based on the dispensability of caspases, a requirement for RIP1 kinase function, and the physiological status of infected cells, we conclude that reovirus can also induce an alternate, necrotic form of cell death described as necroptosis. We also found that induction of necroptosis requires synthesis of viral RNA or proteins, a step distinct from that necessary for the induction of apoptosis. Thus, our studies reveal that two different events in the reovirus replication cycle can injure host cells by distinct mechanisms.**

IMPORTANCE **Virus-induced cell death is a determinant of pathogenesis. Mammalian reovirus is a versatile experimental model for identifying viral and host intermediaries that contribute to cell death and for examining how these factors influence viral disease. In this study, we identified that in addition to apoptosis, a regulated form of cell death, reovirus is capable of inducing an alternate form of controlled cell death known as necroptosis. Death by this pathway perturbs the integrity of host membranes and likely triggers inflammation. We also found that apoptosis and necroptosis following viral infection are activated by distinct mechanisms. Our results suggest that host cells can detect different stages of viral infection and attempt to limit viral replication through different forms of cellular suicide. While these death responses may aid in curbing viral spread, they can also exacerbate tissue injury and disease following infection.**

Received 11 March 2013 **Accepted** 19 April 2013 **Published** 14 May 2013

Citation Berger AK, Danthi P. 2013. Reovirus activates a caspase-independent cell death pathway. mBio 4(3):e00178-13. doi:10.1128/mBio.00178-13

Editor Mary K. Estes, Baylor College of Medicine

Address correspondence to Pranav Danthi, pdanthi@indiana.edu.

Induction of an apoptotic or necrotic form of cell death constitutes an intrinsic response of the host cell to viral infection (1, 2). Though both apoptosis and necrosis function to limit viral infection, they each have markedly different effects on the cell. While apoptosis results in membrane blebbing, nuclear condensation, and DNA fragmentation, the integrity of the plasma membrane is maintained (3). In contrast, necrosis results in cell rounding, cell swelling, and ultimately a loss of plasma membrane integrity, leading to the leakage of host cytoplasmic contents (3). In addition to the morphological differences in dying cells, apoptosis and necrosis also influence host physiology in a distinct manner. While cells dying by apoptosis do not activate the immune system, the leakiness of necrotic cells recruits immune cells and promotes inflammation (4), potentially enhancing pathology associated with cell death. Though necrosis was generally considered to be an unregulated, uncontrolled form of cell death, recent evidence indicates that at least one form of necrosis, necroptosis, is programmed (5). In addition to the leakiness of membranes observed in all forms of necrosis, necroptosis is characterized by the activation of signaling from death receptors, the dispensability of caspase activity, and a requirement for the kinase activity of receptor interacting protein 1 (RIP1 or RIPK1) or 3 (RIP3 or RIPK3) (3). Though both apoptosis and necroptosis have been shown to occur during viral infection, it is not known if similar events in viral infection trigger apoptosis and necroptosis (1). Conditions that favor one form of cell death over the other during viral infection are also not understood.

The importance of apoptosis to viral pathogenesis (6–16) has led to numerous studies to examine the molecular basis of pro-apoptotic signaling following infection with mammalian orthoreovirus, henceforth referred to as reovirus (17). Following receptor-mediated endocytosis, reovirus particles disassemble in the endosome and viral cores are deposited into the cytosol via the function of the viral membrane-penetration protein (17, 18). Steps following escape from the endosome but prior to viral RNA and protein synthesis are required for initiation of the apoptotic pathway (19). This induction process involves the IκB kinase (IKK)-mediated activation of the classical form of the transcription factor NF-κB, comprised of RelA and p50 subunits (20, 21). Activation of NF-κB early following infection is required for the cleavage of the BH3-only member of the Bcl-2 family of mitochondrial proteins, Bid, via the initiator caspase, caspase-8 (14,

22). The cleaved form of Bid, truncated Bid (tBid), amplifies the apoptotic signal through the mitochondria to activate the initiator caspase, caspase-9 (23–25). These events result in activation of the effector caspase, caspase-3, and culminate in cell death. In addition, the protein kinase JNK (c-Jun N-terminal kinase), the cytosolic cysteine protease calpain, and the transcription factor IRF-3 have been shown to contribute to efficient induction of apoptosis by reovirus (26–29). It remains unknown if components of the signaling cascade described above are required for reovirus-induced cell death in all cell types.

In a variety of cell lines, prototype type T3 reovirus strains, T3D and T3A, induce significantly more apoptosis than the type T1 reovirus strain T1L (30–34). In this study, we investigated how T3 and T1 reovirus strains differ in their capacity to evoke cell death. We found that T3D activates NF-κB, initiator caspases, and effector caspases to a greater extent than T1L. Unexpectedly, when T3D-induced NF-κB activation was inhibited, it did not diminish cell death. Caspase inhibitors also failed to block reovirus-induced cell death. Blockade of the kinase activity of RIP1 resulted in a reduction in cell death. Because reovirus-induced cell death in L929 cells fulfills all the criteria that are used to describe necroptosis—activation of death signaling, dispensability of active caspases, the requirement for RIP1 kinase activity, diminishment of cellular ATP levels, and membrane permeability of dying cells (3)—our findings indicate that reovirus is also capable of killing cells by necroptosis. Moreover, we found that induction of this form of cell death following reovirus infection requires *de novo* synthesis of viral mRNA and proteins. These studies therefore highlight a second mechanism by which reovirus infection interfaces with host signal transduction pathways to evoke cell death.

RESULTS

Strain-specific differences in cell death induction correlate with caspase activation. Previous studies have suggested that blockade of the prosurvival function of NF-κB by T3A but not T1L late following infection controls the differences in the capacity of these two strains to elicit apoptosis (34). While following up on these studies, we investigated the extent to which T1L and T3D differ in their capacity to block activation of NF-κB at late times following infection of L929 cells. We found that each strain inhibits tumor necrosis factor alpha (TNF-α)-induced NF-κB nuclear translocation to an equivalent extent (see Fig. S1A in the supplemental material). To determine if T3D and T1L continue to maintain a difference in their capacity to evoke cell death, we performed acridine orange, ethidium bromide (AOEB) staining on infected cells at 48 h after infection. Rather than subjective determination of the staining pattern of the nuclear material to distinguish between apoptotic and necrotic cells (35), all cells that stained with EB were counted as dead cells. Evaluation by this method indicated that T3D induced significantly greater cell death than T1L (Fig. 1A), consistent with previous results (30, 31). Both T1L and T3D were capable of establishing efficient infection in these cells (Fig. S1B). Thus, despite efficiently establishing infection and blocking NF-κB activation late in infection to an equal extent, T3D induced cell death to a much greater extent in L929 cells than did T1L. These data suggest that unlike that reported for HEK293 cells (34), differences in the capacity of T3D and T1L to evoke cell death in L929 cells are not related to inhibition of NF-κB late in infection.

To define how prodeath signaling following T3D and T1L differs, we compared the activations of initiator and executioner caspases following infection of L929 cells by these two strains. Measurement of the activity of the effector caspases, caspase-3 and -7, by chemiluminescent enzymatic assays 24 h after infection indicated that T3D activates these enzymes to a significantly greater extent than T1L (Fig. 1B). Consistent with these results, we found that a greater amount of cleaved caspase-3 was detectable following infection with T3D (see Fig. S1C in the supplemental material). Bid cleavage, a marker for caspase-8 activation following reovirus infection (14), also occurred more efficiently in T3D-infected cells than T1L-infected cells (Fig. S1D). Collectively, these data demonstrate that initiator and effector caspase activity fol-

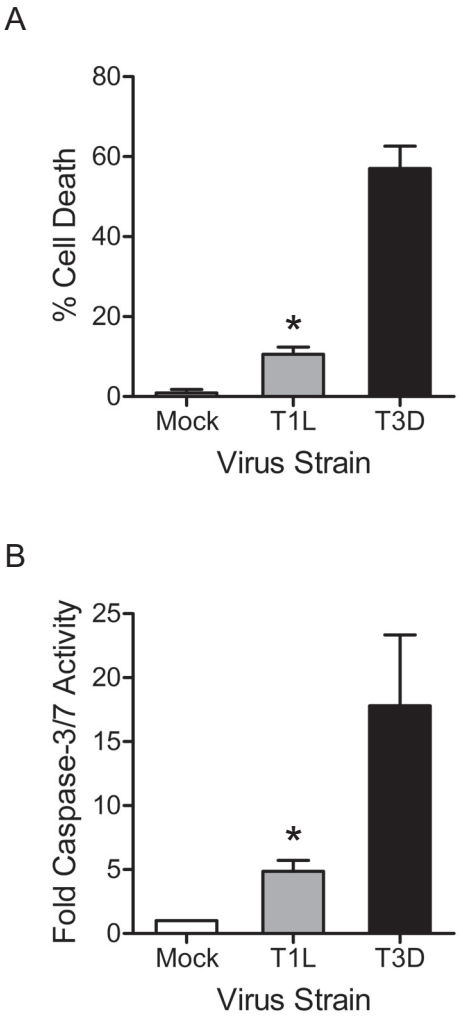

FIG 1 T3D and T1L differ in their efficiency of cell death induction and effector caspase activation. (A) ATCC L929 cells were adsorbed with PBS (mock) or 10 PFU/cell of T3D or T1L. Following incubation at 37°C for 48 h, cells were stained with AOEB. The results are expressed as the mean percentages of cells undergoing cell death for three independent experiments. Error bars indicate standard deviation (SD). *, *P* value of <0.05 as determined by Student's *t* test in comparison to cells infected with T3D. (B) ATCC L929 cells were adsorbed with T3D or T1L at an MOI of 10 PFU/cell or with PBS (mock). After incubation at 37°C for 24 h, caspase-3/7 activity in cell lysates was determined. Results are expressed as the mean ratios of caspase-3/7 activity from infected cell lysates to that from mock-infected cells for triplicate samples. Error bars indicate SD. *, *P* value of <0.05 as determined by Student's *t* test in comparison to cells infected with T3D.

lowing infection of L929 cells with T3D is significantly higher than that following infection with T1L.

Activation of NF-κB is not required for reovirus-induced cell death. Previously, we have suggested that activation of NF-κB early, 6 to 8 h after reovirus infection, is required for caspase-8-mediated generation of tBid and attendant activation of effector caspases (14). To determine if NF-κB activation following infection of L929 cells with T1L and T3D differs, we measured the activation of NF-κB by measuring the loss of IκBα inhibitor from the cytoplasm and the consequent translocation of the NF-κB RelA/p65 subunit to the nucleus (21, 36). Immunoblot analysis of IκBα levels 7.5 h after infection indicates a greater decrease in IκBα levels following infection with T3D than following infection with T1L (Fig. 2A). Consistent with these data, we found a significantly greater level of RelA in the nuclear extracts of T3D-infected cells than in those of T1L-infected cells (Fig. 2B). To test the idea that the enhanced death-inducing potential of T3D in L929 cells may be related to an increased capacity to activate NF-κB, we determined if blockade of NF-κB activation would diminish cell death following T3D infection. For these experiments, we assessed the capacity of T3D to promote cell death in cells treated with an IκBα kinase (IKK) inhibitor, BAY-65-1942 (21, 37). We found that blockade of IKK activation had no effect on the induction of cell death by T3D (Fig. 2C). Treatment of cells with TNF-α in the presence of the IKK inhibitor resulted in cell death, demonstrating that the IKK inhibitor is functional in L929 cells and can block TNF-α-induced prosurvival NF-κB signaling. To ensure that the IKK inhibitor also blocked the unusual IKK complex activated by reovirus (21), we assessed the effect of IKK inhibition on effector caspase activation following reovirus infection. Consistent with the requirement of IKK activity in promoting proapoptotic signaling following reovirus infection (21), we found that in comparison to dimethyl sulfoxide (DMSO)-treated cells, effector caspase activity following reovirus infection was significantly diminished following treatment of cells with the IKK inhibitor (Fig. 2D). Thus, despite blocking proapoptotic signaling following reovirus infection, the IKK inhibitor failed to block reovirus-induced cell death. These studies reveal that T3D is capable of activating a cell death pathway that is not dependent on target gene transcription by NF-κB. Though this observation matches that from primary cardiac myocytes, it is distinct from that reported for other cell types (20, 34, 38). The unexpected dispensability of NF-κB signaling for cell death in L929 cells prompted us to focus on defining the nature of this cell death pathway.

Reovirus induces caspase-independent cell death. Our experiments using the IKK inhibitor suggested that reovirus may induce cell death even in the absence of active effector caspases. To directly test the idea that T3D can evoke cell death in a caspase-independent manner, we assessed cell death 48 h after reovirus infection in the presence of inhibitors of caspase-8 (Z-IETD-FMK) or caspase-9 (Z-LEHD-FMK) or a broad-spectrum inhibitor of caspases [Z-VAD(OMe)-FMK]. Surprisingly, we found that T3D remained capable of inducing cell death in the presence of each of these inhibitors (Fig. 3A). To ensure that the inhibitors were functional in L929 cells at the concentration used, we assessed their capacity to prevent effector caspase activation in T3D-infected cells. For these experiments, caspase-3/7 activity in infected cells treated with each inhibitor was quantified 24 h after infection. We found that in comparison to mock-infected cells, there was an ~10-fold increase in caspase-3/7 activity by infection with T3D in the presence of DMSO (Fig. 3B). Inclusion of inhibitors of caspase-8 or caspase-9 or inclusion of a pan-caspase inhibitor completely blocked effector caspase activation. Thus, despite being capable of blocking the proapoptotic signaling pathway activated by reovirus, these inhibitors failed to prevent virally triggered cell death. These data indicate that reovirus T3D is capable of inducing a distinct cell death pathway in L929 cells that is independent of caspase activation.

Reovirus induces RIP1-dependent necrosis. One such caspase-independent cell death pathway requires the kinase activity of RIP1 (39, 40). To assess whether the caspase-independent cell death pathway activated by reovirus is dependent on the kinase activity of RIP1, we determined the capacity of reovirus to induce cell death following treatment of cells with necrostatin-1 (Nec-1), an inhibitor of RIP1 (41). We found that reovirus-induced cell death was blocked by Nec-1 (Fig. 4A). Simultaneous treatment of cells with Nec-1 and a pan-caspase inhibitor did not further diminish cell death, suggesting that a RIP1 kinase-dependent form of cell death is the primary mechanism of cell death in these cells (Fig. 4A). The effect of Nec-1 on reovirus-induced cell death was independent of its effect on the blockade of indoleamine 2,3-dioxygenase (IDO), an additional target of Nec-1 (42, 43), since direct inhibition of IDO using 1-methyl-L-tryptophan did not prevent reovirus-induced cell death (see Fig. S2A in the supplemental material). The capacity of reovirus to establish infection and grow in Nec-1-treated cells was not affected (Fig. S2B and C). Nec-1 also did not diminish caspase-3/7 activity in T3D-infected cells (Fig. S2D). These data suggest that RIP1 kinase activity is required for reovirus-induced cell death.

Cells undergoing all forms of necrosis, including necroptosis, are characterized by a depletion of cellular ATP levels (44, 45). To determine whether ATP levels were affected in T3D-infected cells, we compared ATP levels over a time course of infection using a chemiluminescent assay. While an ~35% to 40% reduction in ATP was observed at 24 h after infection with T3D, ~75% and ~95% of the ATP was lost in T3D-infected cells at 36 and 48 h after infection, respectively (Fig. 4B). Moreover, the rate at which loss of ATP occurred in T3D-infected cells was diminished by treatment of cells with Nec-1 but not by treatment with a pan-caspase inhibitor. These data provide further support for the idea that T3D-infected L929 cells undergo necroptosis following reovirus infection. Necroptosis alters cellular architecture quite differently from apoptosis. In particular, necroptosis damages the integrity of the plasma membrane. To assess whether plasma membrane integrity was compromised following infection with T3D, we evaluated whether high-mobility group box 1 protein (HMGB1) was released into the medium of infected cells. This protein is not released from apoptotic cells undergoing secondary necrosis, and therefore, leakage of this chromatin-associated protein from cells is considered to be a marker for necrosis (46, 47). We found that HMGB1 was released into the medium at 24 h following infection. A greater level of HMGB1 was detected in the medium at 36 and 48 h after infection with T3D (Fig. 4C). Along with the capacity of EB to gain access and stain the nuclei of unfixed, reovirus-infected cells, a measurement equivalent to propidium iodide or sytox staining of necrotic cells (48), the data presented here indicate that the L929 cell plasma membrane is leaky following infection with T3D. Based on the dispensability of caspases, the requirement for RIP1 kinase activity, the dramatic loss in cellular ATP levels, and the release of HMGB1 from infected cells, we conclude that reo-

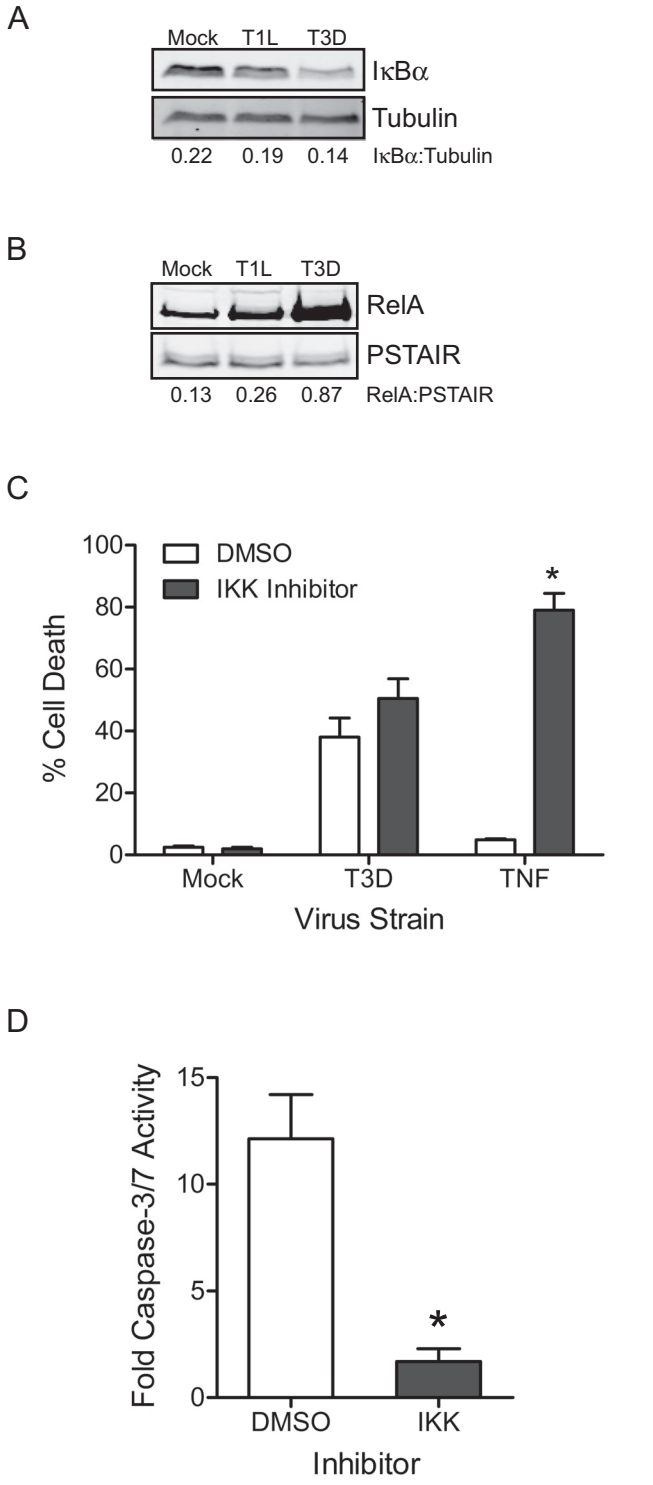

FIG 2 NF-κB is activated but dispensable for induction of cell death. (A) ATCC L929 cells were adsorbed with PBS (mock) or 100 PFU/cell of T3D or T1L. Following incubation at 37°C for 7.5 h, cytoplasmic extracts were immunoblotted using an antiserum specific for IκBα or tubulin. (B) ATCC L929 cells were adsorbed with PBS (mock) or 100 PFU/cell of T3D or T1L. Following incubation at 37°C for 7.5 h, nuclear extracts were immunoblotted using an antiserum specific for RelA or PSTAIR. (C) ATCC L929 cells were adsorbed with PBS (mock) or T3D at an MOI of 10 PFU/cell or treated with 10 ng/ml TNF-α. After incubation at 37°C for 48 h (24 h for TNF-α), in the presence of

(Continued)

virus is capable of inducing an alternate cell death pathway, which has been described as necroptosis.

To determine if infection with T1L also results in necroptosis, we assessed whether ATP is lost from T1L-infected cells. We found that ~30% to 40% ATP was lost after T1L infection at 48 h (see Fig. S3A in the supplemental material). Thus, in comparison to T3D-infected cells (Fig. 4B), ATP loss following infection with T1L is delayed. The loss of ATP in T1L-infected cells was able to be diminished by Nec-1 but not pan-caspase inhibitor treatment, suggesting that cell death following T1L infection also occurs via necroptosis. We also used AOEB staining to determine the kinetics and mechanisms of T1L-induced cell death. We found ~10% and ~30% cell death in cells infected with T1L at 48 and 72 h after infection, respectively (Fig. S3B). Because cell death following T1L infection is sensitive to Nec-1 and is substantially lower than the ~60% cell death induced by T3D at 48 h after infection, our data indicate that T1L induces necroptosis in L929 cells with slower kinetics than T3D.

Induction of necroptosis requires viral RNA or protein synthesis. To define the triggering event in viral infection that ultimately leads to necroptosis, we assessed the requirement for viral genomic RNA and viral replication for induction of necroptosis. To determine whether viral genomic RNA is required for induction of cell death, we infected cells with equivalent numbers of genome-deficient (or top-component) particles and infectious virions and assessed their capacity to elicit cell death. To rule out the effect of secondary rounds of infections from the contaminating infectious particles in the top-component particle fraction, we assessed the induction of cell death at 24 h after infection (19). We found that ~35% and ~20% of the cells were dead following infection with a multiplicity of infection (MOI) of 17,700 particles/cell (equivalent of 100 PFU/cell) or 5,840 particles/cell (equivalent of 33 PFU/cell), respectively, of infectious virus (Fig. 5A). In contrast, infection of cells with an equivalent number of top-component particles killed a substantially smaller amount of cells, ~10% and ~5%, respectively. These data indicate that viral genomic double-stranded RNA (dsRNA) is required for induction of necroptosis.

To determine if genomic dsRNA is sufficient to trigger necroptosis, we assessed the capacity of UV-inactivated virus to evoke cell death. UV-inactivated reovirus contains genomic dsRNA, but the RNA is not competent to serve as a template for viral mRNA synthesis. We observed that UV-treated reovirus particles had a significantly lower capacity for inducing cell death than an equivalent dose of infectious virus (Fig. 5B). These findings indicate that genomic dsRNA within incoming virus particles is insufficient to evoke necroptosis in infected cells and suggest that *de novo*

Figure Legend Continued

DMSO or a 5 μM concentration of the IKK inhibitor BAY-65-1942, the cells were stained with AOEB. The results are expressed as the mean percentages of cells undergoing cell death for three independent experiments. Error bars indicate SD. *, *P* value of <0.05 as determined by Student's *t* test in comparison to cells treated with TNF-α. (D) ATCC L929 cells were adsorbed with PBS (mock) or T3D at an MOI of 10 PFU/cell in the presence of DMSO or a 5 μM concentration of the IKK inhibitor BAY-65-1942. After incubation at 37°C for 24 h, caspase-3/7 activity in cell lysates was determined. Results are expressed as the mean ratios of caspase-3/7 activity from infected cell lysates to that from equivalently treated mock-infected cells for triplicate samples. Error bars indicate SD. *, *P* value of <0.05 as determined by Student's *t* test in comparison to T3D-infected cells treated with DMSO.

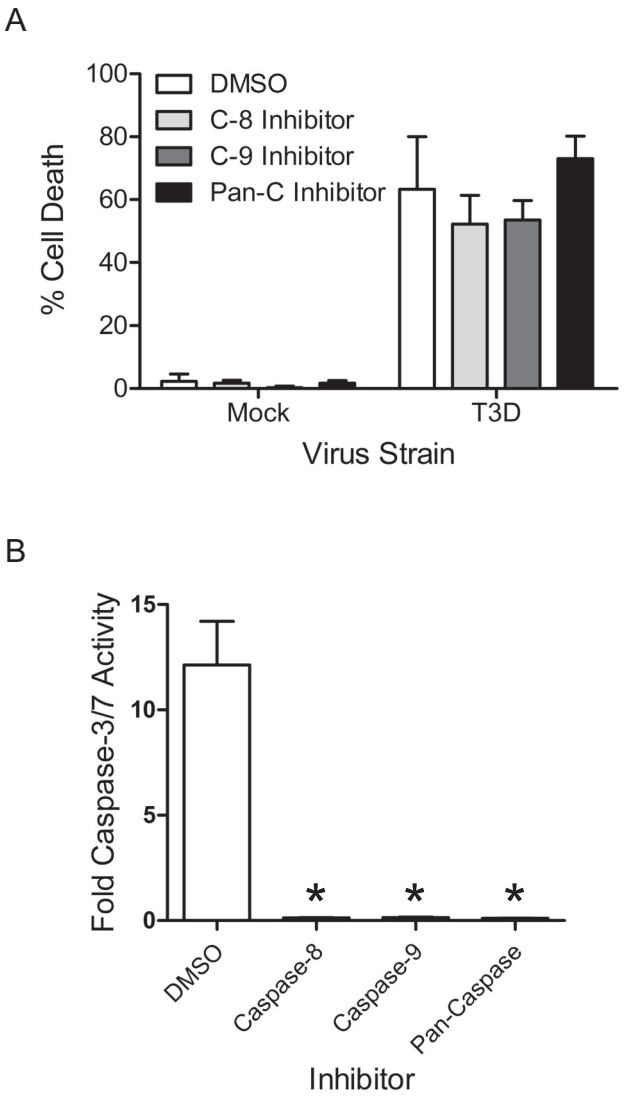

FIG 3 Caspase activity is not required for T3D-induced cell death. (A) ATCC L929 cells were adsorbed with PBS (mock) or T3D at an MOI of 10 PFU/cell. After incubation at 37°C for 48 h in the presence of DMSO or 25 μM caspase-8 (Z-IETD-FMK), caspase-9 (Z-LEHD-FMK), or pan-caspase [Z-VAD(OMe)-FMK] inhibitor, cells were stained with AOEB. The results are expressed as the mean percentages of cells undergoing cell death for three independent experiments. Error bars indicate SD. (B) ATCC L929 cells were adsorbed with PBS (mock) or T3D at the MOI of 10 PFU/cell. After incubation at 37°C for 24 h in the presence of DMSO or 25 μM concentrations of each caspase inhibitor, caspase-3/7 activity in cell lysates was determined. Results are expressed as the mean ratios of caspase-3/7 activity from infected cell lysates to that from equivalently treated mock-infected cells for triplicate samples. We note that the DMSO-treated cells are the same as those used in Fig. 2. Error bars indicate SD. *, P value of <0.05 as determined by Student's t test in comparison to T3D-infected cells treated with DMSO.

synthesis of viral RNA is required for induction of necroptosis following reovirus infection. Since viral genomic RNA and virus replication are dispensable for induction of apoptosis (19, 49), these findings suggest that apoptosis and necroptosis following reovirus infection are initiated at different stages of viral infection.

DISCUSSION

Reovirus-induced apoptotic cell death has been extensively investigated (see Fig. S4 in the supplemental material). On examination of strain-specific differences in the cell death pathways activated by reovirus, we made a surprising observation that reovirus was capable of inducing cell death even in the absence of NF-κB signaling and active caspases. We found that T3D-induced cell death requires the function of RIP1 kinase, results in a drop in cellular ATP levels, and renders the host cell plasma membrane leaky. These data indicate that in addition to apoptosis, reovirus is also capable of inducing necroptosis following viral infection. We also found that induction of the necroptosis pathway following reovirus infection occurs later in infection and requires the *de novo* synthesis of viral RNA or proteins.

RIP1-dependent necroptosis pathways are initiated via at least three different mechanisms. One pathway for initiation of necroptosis is dependent on death receptor signaling (50). Experiments presented here and in several other studies indicate that death receptor signaling is activated following reovirus infection (14, 22, 51). While this observation may suggest that necroptosis following reovirus infection may be a consequence of death receptor signaling, our findings using the IKK inhibitor, which fails to inhibit necroptosis despite blocking classical apoptotic pathways, argues against this idea. An alternate pathway for the induction of necroptosis involves recognition of pathogen-associated molecular patterns by pattern recognition receptors. Among these, TLR3, a sensor of dsRNA, and DNA-dependent activator of interferon regulatory factor (DAI), a sensor of dsDNA, have been implicated in initiating necroptosis following viral infection (52, 53). Based on the requirement for viral genomic RNA and for viral replication, our data may suggest a role for TLR3-mediated detection of viral RNA in induction of necroptosis in these cells. If so, it remains to be determined how viral genomic RNA within the reovirus core or viral mRNA, which is present in the cytoplasm, may be detected by endosomally localized TLR3. A third pathway for necroptosis is thought to occur independently from Toll-like receptor (TLR) or death receptor signaling and requires the loss of inhibitors of apoptosis (IAPs) (52). Interestingly, there is evidence for the loss of IAPs during reovirus infection (25). Thus, it is possible that necroptosis following reovirus infection may be initiated by any of these pathways. It is also possible that one of the eleven reovirus proteins synthesized by translation of viral mRNA triggers this death response. Our ongoing studies are targeted toward understanding how necroptosis is triggered by reovirus infection and how strains T3D and T1L differ in their capacity to evoke necroptosis.

Induction of necroptosis by any of the pathways described above requires the formation of the ripoptosome or a similar multiprotein complex (54). This 2-MDa signaling complex is comprised of three core components, RIP1, caspase-8, and FADD (54). In addition, it also contains regulators such as cFLIP, cIAP1, cIAP2, and XIAP. The decision between cell survival, apoptosis, and necroptosis occurs at the level of the ripoptosome and depends on the activity of caspase-8 (40). When procaspase-8 is sufficiently processed and caspase-8 activity is high, apoptosis ensues. In contrast, when caspase-8 activity is lower due to heterodimerization of caspase-8 with $cFLIP_L$, no apoptosis occurs. Under these conditions, caspase-8-$cFLIP_L$ complexes retain sufficient activity to cleave RIP1, preventing necroptosis. Thus, when

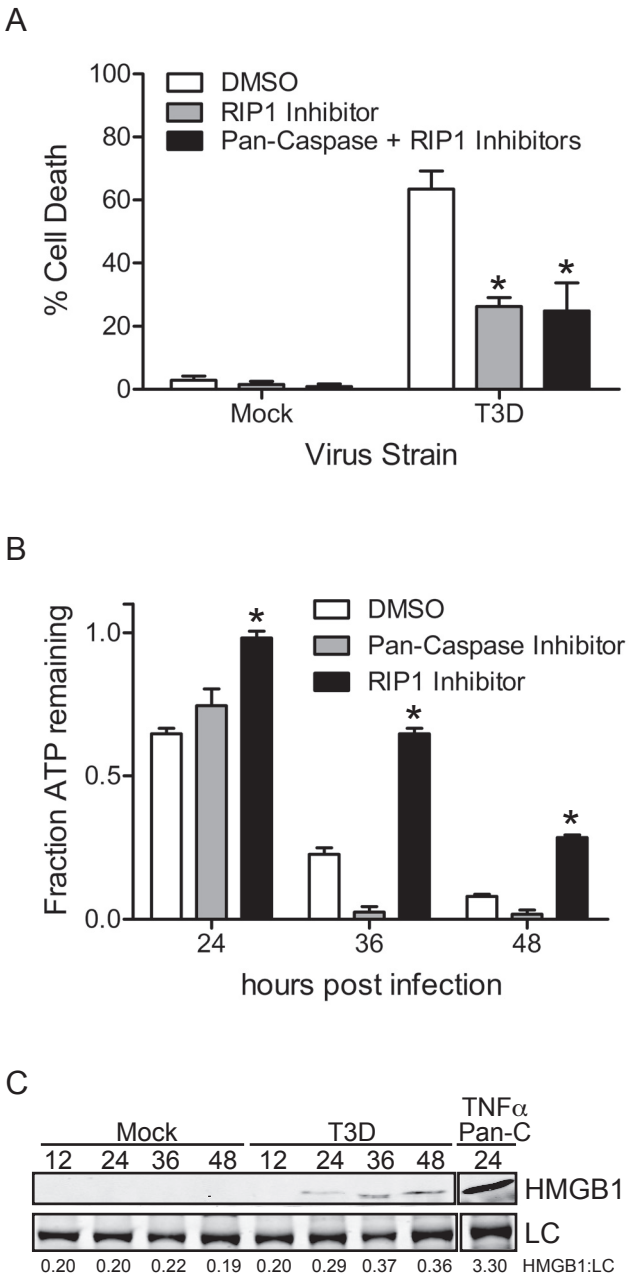

FIG 4 T3D-induced cell death exhibits characteristics of necroptosis. (A) ATCC L929 cells were adsorbed with T3D at an MOI of 10 PFU/cell. After incubation at 37°C for 48 h in the presence of DMSO, 50 μM RIP1 inhibitor (Nec-1), or a combination of 50 μM RIP1 inhibitor (Nec-1) and 25 μM pan-caspase inhibitor [Z-VAD(OMe)-FMK], cells were harvested and stained with AOEB. The results are expressed as the mean percentages of cells undergoing cell death for three independent experiments. Error bars indicate SD. *, *P* value of <0.05 as determined by Student's *t* test in comparison to T3D-infected cells treated with DMSO. (B) ATCC L929 cells were adsorbed with PBS (mock) or 10 PFU/cell of T3D. Following incubation at 37°C for the indicated amount of time, ATP levels in cells treated with DMSO, pan-caspase inhibitor, or RIP1 inhibitor were measured. Results are expressed as the mean ratios of ATP from mock-infected cells to that from equivalently treated T3D-infected cells for triplicate samples. Error bars indicate SD. *, *P* value of <0.05 as determined by Student's *t* test in comparison to T3D-infected cells treated with DMSO. (C) ATCC L929 cells were adsorbed with PBS (mock) or 10 PFU/cell of T3D. Following incubation at 37°C for the indicated amount of time, DNase-treated medium from infected cells was resolved by SDS-PAGE and immunoblotted using an antiserum specific for HMGB1. An ~200-kDa band of unknown

(Continued)

activity of caspase-8 is low, cells survive. If, instead, caspase-8 is blocked by binding to $cFLIP_L$ or the presence of cIAPs, RIP1 is not cleaved and the cells undergo necroptosis. Thus, we should anticipate that when caspase-8 is active, reovirus infection results in apoptosis, and when it is inhibited, by inclusion of caspase-8 or pan-caspase inhibitor, reovirus infection produces necroptosis. In our studies, reovirus-induced cell death was sensitive to Nec-1 even in the absence of treatment with caspase inhibitors. These data suggest that the activity of caspase-8 following reovirus infection is not sufficient to cleave and inactivate RIP1, thereby allowing induction of necroptosis.

Though reovirus-induced cell death has been extensively examined in a variety of cell lines (8, 20, 30–34, 49, 55–57), this is the first demonstration of necroptosis following reovirus infection. One possible reason for why this observation has not been previously reported is that prior studies on reovirus apoptosis, including our own, have not examined this possibility. In the majority of studies, cell death following reovirus infection has been considered apoptotic due to the presence of morphological and biochemical features, but the effect of treatments that block cell death has been evaluated in some (8, 14, 32, 58) but not all (27–31, 51) cell types. Alternatively, it is possible that this pathway has been discovered in L929 cells due to peculiarities in the amounts or activities of proteins that regulate various forms of cell death. Because L929 cells are among the most permissive to reovirus infection, a related possibility is that reovirus alters the levels of these signaling or regulatory molecules differently or to a different extent than in other cell types. Regardless, our data indicate that necroptosis following reovirus infection is an alternate mechanism of cell death.

Analogous to studies on reovirus-induced apoptosis (14, 20, 21), we found no effect of inhibition of necroptosis on reovirus replication (see Fig. S2 in the supplemental material). Thus, regardless of whether reovirus induces necroptosis in other cultured cell lines, the physiological relevance of necroptosis to reovirus infection can be determined only by *in vivo* experiments, as has been necessary for the demonstration of the pathogenic role of reovirus-induced apoptosis (7–12, 14–16, 59). T3 reoviruses cause bile duct injury, leading to biliary atresia (60–63). Histological examination of the reovirus-infected bile ducts has revealed the presence of necrotic tissue (61, 62). Some studies on reovirus-induced myocarditis also report the presence of necrotic lesions (12, 13, 64). Consistent with the induction of the necrotic form of cell death, inflammatory cells are detected in the injured tissues (12, 13, 61, 62). In each of these cases, it is not clear if the necrotic tissue observed is secondary necrosis as a consequence of apoptosis or whether direct induction of necrosis contributes to cell death in these tissues. In at least two of these studies (12, 13), cell death in the infected tissue appears to occur even in the absence of molecules previously shown to be required for apoptosis in cultured cells (20, 26), suggesting the existence of alternate mechanisms of cell death. Further work is needed to determine whether this alternate form of cell death is indeed necrotic and occurs via a

Figure Legend Continued

origin found in medium from infected cells, resolved by SDS-PAGE, and stained using Coomassie blue staining was used as a loading control (LC). Cells treated with TNF-α and pan-caspase inhibitor were used as a necroptosis control.

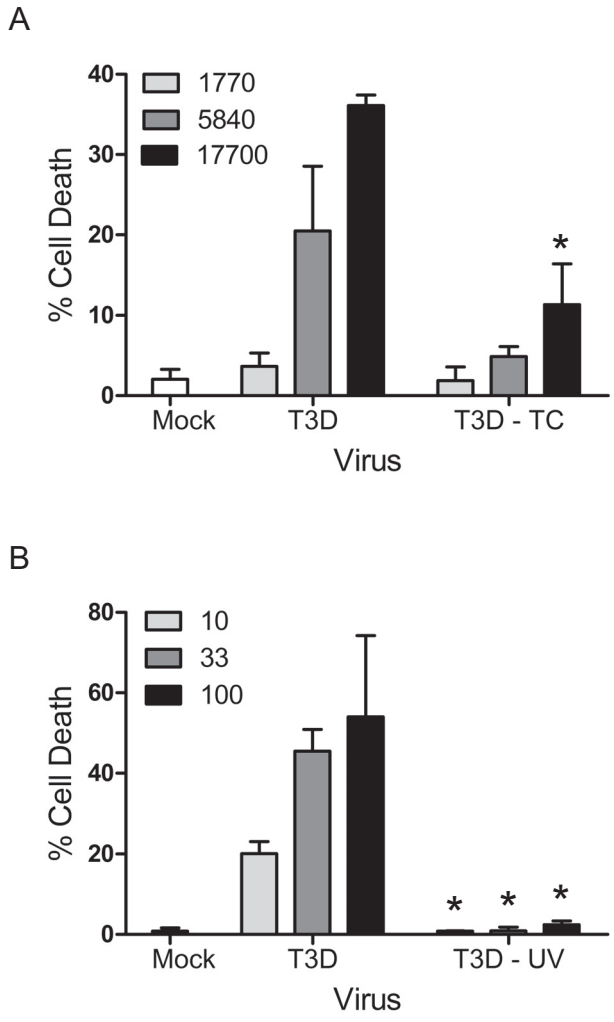

FIG 5 Viral RNA and protein synthesis are required for induction of necroptosis. (A) ATCC L929 cells were adsorbed with PBS (mock) or an equivalent number of genome-containing (T3D) or genome-deficient, top-component (T3D-TC) virus particles. After incubation at 37°C for 24 h, cells were stained with AOEB. The results are expressed as the mean percentages of cells undergoing cell death for three independent experiments. Error bars indicate SD. *, *P* value of <0.05 as determined by Student's *t* test in comparison to T3D-infected cells at an equivalent MOI. (B) ATCC L929 cells were adsorbed with PBS (mock) or T3D at indicated MOIs or with UV-inactivated T3D (T3D-UV) at equivalent MOIs before irradiation. After incubation at 37°C for 24 h, cells were stained with AOEB. The results are expressed as the mean percentages of cells undergoing cell death for three independent experiments. Error bars indicate SD. *, *P* value of <0.05 as determined by Student's *t* test in comparison to T3D-infected cells at an equivalent MOI.

caspase-independent, RIP1-dependent pathway that we have identified here. Such studies will enhance our understanding of reovirus pathogenesis.

The two forms of programmed cell death pathways observed following reovirus infection, apoptosis and necroptosis, are part of the intrinsic host defense response (1, 2). Analogous to a few other viruses (65–73), apoptosis following reovirus infection is activated prior to synthesis of the viral RNA by the proteinaceous components of the incoming viral capsid (15, 16, 19, 49). Though there are fewer studies that indicate how necroptosis is initiated following virus infection, extant information and our findings presented here indicate that necroptosis is initiated later in infection following synthesis of new viral genomes or gene products (53, 74–76). Based on these findings, we propose that apoptosis and necroptosis are two complementary mechanisms that sense and respond to different stages of pathogen invasion with a common goal of limiting viral infection through cellular suicide.

MATERIALS AND METHODS

Cells and viruses. Murine L929 cells (ATCC CCL-1) were maintained in Eagle's minimal essential medium (MEM) (Lonza) supplemented with 5% fetal bovine serum (FBS) and 2 mM L-glutamine. Spinner-adapted L929 cells (obtained from T. Dermody's laboratory) were maintained in Joklik's MEM (Lonza) supplemented to contain 5% FBS, 2 mM L-glutamine, 100 U/ml of penicillin, 100 μg/ml of streptomycin, and 25 ng/ml of amphotericin B. Spinner-adapted L929 cells were used for cultivating and purifying viruses and for plaque assays. ATCC L929 cells were used for all experiments to assess cell death and cell signaling. No differences were observed in permissivity between ATCC L929 cells and spinner-adapted L929 cells. Prototype reovirus strains T1L and T3D were regenerated by plasmid-based reverse genetics (77, 78). No reverse genetic system is available for T3A, and thus, a laboratory stock was used. Infectious and genome-deficient viral particles were purified by Vertrel XF extraction and CsCl gradient centrifugation (79). Viral titer was determined by a plaque assay using spinner-adapted L929 cells (80). UV-inactivated virus was generated using a UV cross-linker (CL-1000 UV Crosslinker; UVP). T3D virus (1×10^9 PFU/ml) was irradiated with short-wave (254-nm) UV on ice at a distance of 10 cm for 1 min at 120,000 μJ/cm^2 in a 60-mm tissue culture dish. Particle numbers for top-component and infectious virus were determined by estimating the protein concentration in each sample. One hundred eighty-five micrograms of protein was considered equal to 2.1×10^{12} virions (81). Relative per-particle infectivity of intact, genome-deficient virions and UV-inactivated virions was determined using indirect immunofluorescence.

Antibodies and reagents. Antisera raised against T3D, T1L, and σNS have been described (82, 83). Rabbit antisera specific for cleaved caspase-3 and HMGB1 were purchased from Cell Signaling, rabbit antisera specific for RelA and IκBα were purchased from Santa Cruz Biotechnology, and rabbit antiserum against poly(ADP-ribose) polymerase (PARP) was purchased from Roche. Goat antiserum specific for Bid was purchased from R&D Systems. Mouse antisera specific for tubulin and PSTAIR were purchased from Sigma. Alexa Fluor-conjugated anti-mouse IgG, anti-rabbit IgG, and anti-goat IgG secondary antibodies were purchased from Invitrogen. IRDye-conjugated anti-guinea pig IgG was purchased from LI-COR. TNF-α was purchased from Sigma and used at a concentration of 10 ng/ml. Inhibitors of caspase-8 and -9 (Z-IETD-FMK and Z-LEHD-FMK), purchased from R&D Systems, and a broad-spectrum caspase inhibitor [Z-VAD(OMe)-FMK], purchased from Santa Cruz Biotechnologies, were used at a concentration of 25 μM. The RIP1 inhibitor necrostatin-1 was purchased from Santa Cruz Biotechnologies and used at a concentration of 50 μM. IKK inhibitor, described by Bayer (BAY-45-1962) (37), was used at a concentration of 5 μM. The IDO inhibitor 1-methyl-L-tryptophan (1-MT) was purchased from Sigma and used at 10 and 100 μM. As shown in the respective experiments, none of the inhibitors displayed any cytotoxicity at the concentration used.

Infections and preparation of extracts. ATCC L929 cells were adsorbed with either phosphate-buffered saline (PBS) or reovirus at the indicated MOI at room temperature for 1 h, followed by incubation with medium at 37°C for the indicated time interval. For assessment of NF-κB activation, serum-starved cells were infected in the presence of serum-free medium. All inhibitors were added to cells in medium 1 h before virus adsorption and returned with medium after the 1-h adsorption period. For preparation of whole-cell lysates, cells were washed in phosphate-buffered saline (PBS) and lysed with 1× RIPA (50 mM Tris [pH 7.5], 50 mM NaCl, 1% TX-100, 1% deoxycholate, 0.1% SDS, and 1 mM EDTA)

containing a protease inhibitor cocktail (Roche), 500 μM dithiothreitol (DTT), and 500 μM phenylmethylsulfonyl fluoride (PMSF), followed by centrifugation at 15,000 $\times$ *g* for 10 min to remove debris. Nuclear and cytoplasmic extracts were prepared by hypotonic lysis and high salt extraction, respectively, as previously described (20, 21).

Immunoblot assay. The cell lysates or extracts were resolved by electrophoresis in polyacrylamide gels and transferred to nitrocellulose membranes. Membranes were blocked for at least 1 h in blocking buffer (PBS containing 5% milk or 2.5% bovine serum albumin [BSA]) and incubated with antisera against Bid (1:1,000), RelA (1:1,000), IκBα (1:500), σNS (1:750), cleaved caspase-3 (1:500), PARP (1:1,000), HMGB1 (1:500), tubulin (1:500), or PSTAIR (1:10,000) at 4°C overnight. Membranes were washed three times for 5 min each with washing buffer (Tris-buffered saline [TBS] containing 0.1% Tween-20) and incubated with a 1:20,000 dilution of Alexa Fluor-conjugated goat anti-rabbit Ig (for RelA, IκBα, caspase-3, HMGB1, and PARP), goat anti-mouse Ig (for PSTAIR and tubulin), donkey anti-goat Ig (for Bid), or IRDye-conjugated anti-guinea pig IgG (for σNS) in blocking buffer. Following three washes, membranes were scanned and quantified using an Odyssey infrared Imager (LI-COR).

Quantitation of cell death by AOEB staining. ATCC L929 cells (2×10^5) grown in 24-well plates were adsorbed with the indicated MOI of reovirus at room temperature for 1 h. The percentage of dead cells after 24, 48, or 72 h incubation was determined using AOEB staining as described previously (30). For each experiment, >100 cells were counted, and the percentage of isolated cells exhibiting orange staining (EB positivity) was determined by epi-illumination fluorescence microscopy using a fluorescein filter set on an Olympus IX71 microscope.

Assessment of caspase-3/7 activity. ATCC L929 cells (2×10^4) were seeded into black, clear-bottom 96-well plates and adsorbed with 10 PFU/cell of reovirus in serum-free medium at room temperature for 1 h. Following incubation of cells at 37°C for 24 h, caspase-3/7 activity was quantified using the Caspase-Glo-3/7 assay system (Promega).

Assessment of cellular ATP levels. ATCC L929 cells (2×10^4) were seeded into 96-well plates and adsorbed with 10 PFU/cell of reovirus in serum-free medium at room temperature for 1 h. Following incubation of cells at 37°C for the indicated time interval, ATP levels were assessed in opaque white 96-well plates using the CellTiter-Glo assay system (Promega).

Assessment of viral infectivity by indirect immunofluorescence. ATCC L929 cells (5×10^4) in 96-well plates were adsorbed with 2 PFU/cell of reovirus at room temperature for 1 h. Following incubation at 37°C for 18 h, reovirus-infected cells were visualized by indirect immunofluorescence using an Olympus IX71 fluorescence microscope as described previously (15). Reovirus antigen-positive cells were quantified by counting fluorescent cells in at least two random fields of view in duplicate wells at a magnification of 16×.

Assessment of viral replication by plaque assay. ATCC L929 cells (2×10^5) in 24-well plates were adsorbed with 2 PFU/cell of T3D at room temperature for 1 h. Cells were washed once with PBS, and medium with DMSO or RIP1 inhibitor was added. Cells were frozen immediately or following infection for 24 h. Cells were frozen and thawed twice before determination of titer by plaque assay using spinner L929 cells. Viral yields were calculated according to the following formula: $\log_{10}$ yield = $\log_{10}(\text{PFU/ml})_{24\text{ h}} - \log_{10}(\text{PFU/ml})_{0\text{ h}}$.

SUPPLEMENTAL MATERIAL

Supplemental material for this article may be found at http://mbio.asm.org/lookup/suppl/doi:10.1128/mBio.00178-13/-/DCSupplemental.

Figure S1, EPS file, 1.6 MB.
Figure S2, EPS file, 7.2 MB.
Figure S3, EPS file, 5.8 MB.
Figure S4, EPS file, 0.8 MB.

ACKNOWLEDGMENTS

This research was supported by the American Heart Association Midwest Affiliate award 09SDG2140019 (to P.D.) and startup funds from Indiana University. A.K.B. was supported by Public Health Service award T32 GM007757.

We thank members of our laboratory, Karl Boehme, Geoff Holm, Tuli Mukhopadhyay, and Michael Roner, for helpful suggestions or review of the manuscript.

REFERENCES

1. **Mocarski ES, Upton JW, Kaiser WJ.** 2012. Viral infection and the evolution of caspase 8-regulated apoptotic and necrotic death pathways. Nat. Rev. Immunol. **12**:79–88.
2. **Lamkanfi M, Dixit VM.** 2010. Manipulation of host cell death pathways during microbial infections. Cell Host Microbe **8**:44–54.
3. **Galluzzi L, Vitale I, Abrams JM, Alnemri ES, Baehrecke EH, Blagosklonny MV, Dawson TM, Dawson VL, El-Deiry WS, Fulda S, Gottlieb E, Green DR, Hengartner MO, Kepp O, Knight RA, Kumar S, Lipton SA, Lu X, Madeo F, Malorni W, Mehlen P, Nuñez G, Peter ME, Piacentini M, Rubinsztein DC, Shi Y, Simon HU, Vandenabeele P, White E, Yuan J, Zhivotovsky B, Melino G, Kroemer G.** 2012. Molecular definitions of cell death subroutines: recommendations of the Nomenclature Committee on Cell Death 2012. Cell Death Differ. **19**:107–120.
4. **Kono H, Rock KL.** 2008. How dying cells alert the immune system to danger. Nat. Rev. Immunol. **8**:279–289.
5. **Hitomi J, Christofferson DE, Ng A, Yao J, Degterev A, Xavier RJ, Yuan J.** 2008. Identification of a molecular signaling network that regulates a cellular necrotic cell death pathway. Cell **135**:1311–1323.
6. **Richardson-Burns SM, Tyler KL.** 2004. Regional differences in viral growth and central nervous system injury correlate with apoptosis. J. Virol. **78**:5466–5475.
7. **Oberhaus SM, Smith RL, Clayton GH, Dermody TS, Tyler KL.** 1997. Reovirus infection and tissue injury in the mouse central nervous system are associated with apoptosis. J. Virol. **71**:2100–2106.
8. **DeBiasi RL, Robinson BA, Sherry B, Bouchard R, Brown RD, Rizeq M, Long C, Tyler KL.** 2004. Caspase inhibition protects against reovirus-induced myocardial injury in vitro and in vivo. J. Virol. **78**:11040–11050.
9. **Clarke P, Beckham JD, Leser JS, Hoyt CC, Tyler KL.** 2009. Fas-mediated apoptotic signaling in the mouse brain following reovirus infection. J. Virol. **83**:6161–6170.
10. **Berens HM, Tyler KL.** 2011. The proapoptotic Bcl-2 protein Bax plays an important role in the pathogenesis of reovirus encephalitis. J. Virol. **85**:3858–3871.
11. **Beckham JD, Goody RJ, Clarke P, Bonny C, Tyler KL.** 2007. A novel strategy for the treatment of viral CNS infection utilizing a cell-permeable inhibitor of c-Jun N-terminal kinase. J. Virol. **81**:6984–6992.
12. **O'Donnell SM, Hansberger MW, Connolly JL, Chappell JD, Watson MJ, Pierce JM, Wetzel JD, Han W, Barton ES, Forrest JC, Valyi-Nagy T, Yull FE, Blackwell TS, Rottman JN, Sherry B, Dermody TS.** 2005. Organ-specific roles for transcription factor NF-κB in reovirus-induced apoptosis and disease. J. Clin. Invest. **115**:2341–2350.
13. **Holm GH, Pruijssers AJ, Li L, Danthi P, Sherry B, Dermody TS.** 2010. Interferon regulatory factor-3 attenuates reovirus myocarditis and contributes to viral clearance. J. Virol. **84**:6900–6908.
14. **Danthi P, Pruijssers AJ, Berger AK, Holm GH, Zinkel SS, Dermody TS.** 2010. Bid regulates the pathogenesis of neurotropic reovirus. PLoS Pathog. **6**:e1000980. http://dx.doi.org/10.1371/journal.ppat.1000980.
15. **Danthi P, Kobayashi T, Holm GH, Hansberger MW, Abel TW, Dermody TS.** 2008. Reovirus apoptosis and virulence are regulated by host cell membrane penetration efficiency. J. Virol. **82**:161–172.
16. **Danthi P, Coffey CM, Parker JS, Abel TW, Dermody TS.** 2008. Independent regulation of reovirus membrane penetration and apoptosis by the mu1 phi domain. PLoS Pathog. **4**:e1000248. http://dx.doi.org/10.1371/journal.ppat.1000248.
17. **Danthi P, Holm GH, Stehle T, Dermody TS.** 2013. Reovirus receptors, cell entry, and signaling, p 1–30. *In* Pöhlmann S, Simmons G (ed), Viral entry into cells. Landes Bioscience, Georgetown, TX.
18. **Danthi P, Guglielmi KM, Kirchner E, Mainou B, Stehle T, Dermody TS.** 2010. From touchdown to transcription: the reovirus cell entry pathway. Curr. Top. Microbiol. Immunol. **343**:91–119.
19. **Connolly JL, Dermody TS.** 2002. Virion disassembly is required for apoptosis induced by reovirus. J. Virol. **76**:1632–1641.
20. **Connolly JL, Rodgers SE, Clarke P, Ballard DW, Kerr LD, Tyler KL, Dermody TS.** 2000. Reovirus-induced apoptosis requires activation of transcription factor NF-κB. J. Virol. **74**:2981–2989.

21. **Hansberger MW, Campbell JA, Danthi P, Arrate P, Pennington KN, Marcu KB, Ballard DW, Dermody TS.** 2007. IκB kinase subunits α and γ are required for activation of NF-κB and induction of apoptosis by mammalian reovirus. J. Virol. **81**:1360–1371.
22. **Kominsky DJ, Bickel RJ, Tyler KL.** 2002. Reovirus-induced apoptosis requires both death receptor- and mitochondrial-mediated caspase-dependent pathways of cell death. Cell Death Differ. **9**:926–933.
23. **Luo X, Budihardjo I, Zou H, Slaughter C, Wang X.** 1998. Bid, a Bcl2 interacting protein, mediates cytochrome *c* release from mitochondria in response to activation of cell surface death receptors. Cell **94**:481–490.
24. **Li H, Zhu H, Xu CJ, Yuan J.** 1998. Cleavage of BID by caspase 8 mediates the mitochondrial damage in the Fas pathway of apoptosis. Cell **94**: 491–501.
25. **Kominsky DJ, Bickel RJ, Tyler KL.** 2002. Reovirus-induced apoptosis requires mitochondrial release of Smac/DIABLO and involves reduction of cellular inhibitor of apoptosis protein levels. J. Virol. **76**:11414–11424.
26. **Holm GH, Zurney J, Tumilasci V, Leveille S, Danthi P, Hiscott J, Sherry B, Dermody TS.** 2007. Retinoic acid-inducible gene-I and interferon-beta promoter stimulator-1 augment proapoptotic responses following mammalian reovirus infection via interferon regulatory factor-3. J. Biol. Chem. **282**:21953–21961.
27. **Debiasi RL, Squier MK, Pike B, Wynes M, Dermody TS, Cohen JJ, Tyler KL.** 1999. Reovirus-induced apoptosis is preceded by increased cellular calpain activity and is blocked by calpain inhibitors. J. Virol. **73**: 695–701.
28. **Clarke P, Meintzer SM, Wang Y, Moffitt LA, Richardson-Burns SM, Johnson GL, Tyler KL.** 2004. JNK regulates the release of proapoptotic mitochondrial factors in reovirus-infected cells. J. Virol. **78**:13132–13138.
29. **Clarke P, Meintzer SM, Widmann C, Johnson GL, Tyler KL.** 2001. Reovirus infection activates JNK and the JNK-dependent transcription factor c-Jun. J. Virol. **75**:11275–11283.
30. **Tyler KL, Squier MK, Rodgers SE, Schneider BE, Oberhaus SM, Grdina TA, Cohen JJ, Dermody TS.** 1995. Differences in the capacity of reovirus strains to induce apoptosis are determined by the viral attachment protein sigma 1. J. Virol. **69**:6972–6979.
31. **Tyler KL, Squier MK, Brown AL, Pike B, Willis D, Oberhaus SM, Dermody TS, Cohen JJ.** 1996. Linkage between reovirus-induced apoptosis and inhibition of cellular DNA synthesis: role of the S1 and M2 genes. J. Virol. **70**:7984–7991.
32. **Rodgers SE, Barton ES, Oberhaus SM, Pike B, Gibson CA, Tyler KL, Dermody TS.** 1997. Reovirus-induced apoptosis of MDCK cells is not linked to viral yield and is blocked by Bcl-2. J. Virol. **71**:2540–2546.
33. **Connolly JL, Barton ES, Dermody TS.** 2001. Reovirus binding to cell surface sialic acid potentiates virus-induced apoptosis. J. Virol. **75**: 4029–4039.
34. **Clarke P, Debiasi RL, Meintzer SM, Robinson BA, Tyler KL.** 2005. Inhibition of NF-kappa B activity and cFLIP expression contribute to viral-induced apoptosis. Apoptosis **10**:513–524.
35. **Ribble D, Goldstein NB, Norris DA, Shellman YG.** 2005. A simple technique for quantifying apoptosis in 96-well plates. BMC Biotechnol. **5**:12.
36. **Hayden MS, Ghosh S.** 2004. Signaling to NF-kappaB. Genes Dev. **18**: 2195–2224.
37. **Ziegelbauer K, Gantner F, Lukacs NW, Berlin A, Fuchikami K, Niki T, Sakai K, Inbe H, Takeshita K, Ishimori M, Komura H, Murata T, Lowinger T, Bacon KB.** 2005. A selective novel low-molecular-weight inhibitor of IκB kinase-beta (IKK-beta) prevents pulmonary inflammation and shows broad anti-inflammatory activity. Br. J. Pharmacol. **145**: 178–192.
38. **Clarke P, Meintzer SM, Moffitt LA, Tyler KL.** 2003. Two distinct phases of virus-induced nuclear factor kappa B regulation enhance tumor necrosis factor-related apoptosis-inducing ligand-mediated apoptosis in virus-infected cells. J. Biol. Chem. **278**:18092–18100.
39. **Festjens N, Vanden Berghe T, Cornelis S, Vandenabeele P.** 2007. RIP1, a kinase on the crossroads of a cell's decision to live or die. Cell Death Differ. **14**:400–410.
40. **Vandenabeele P, Galluzzi L, Vanden Berghe T, Kroemer G.** 2010. Molecular mechanisms of necroptosis: an ordered cellular explosion. Nat. Rev. Mol. Cell Biol. **11**:700–714.
41. **Degterev A, Hitomi J, Germscheid M, Ch'en IL, Korkina O, Teng X, Abbott D, Cuny GD, Yuan C, Wagner G, Hedrick SM, Gerber SA, Lugovskoy A, Yuan J.** 2008. Identification of RIP1 kinase as a specific cellular target of necrostatins. Nat. Chem. Biol. **4**:313–321.
42. **Degterev A, Maki JL, Yuan J.** 2013. Activity and specificity of necrostatin-1, small-molecule inhibitor of RIP1 kinase. Cell Death Differ. **20**:366.
43. **Takahashi N, Duprez L, Grootjans S, Cauwels A, Nerinckx W, DuHadaway JB, Goossens V, Roelandt R, Van Hauwermeiren F, Libert C, Declercq W, Callewaert N, Prendergast GC, Degterev A, Yuan J, Vandenabeele P.** 2012. Necrostatin-1 analogues: critical issues on the specificity, activity and in vivo use in experimental disease models. Cell Death Dis. **3**:e437. http://dx.doi.org/10.1038/cddis.2012.176.
44. **Golstein P, Kroemer G.** 2007. Cell death by necrosis: towards a molecular definition. Trends Biochem. Sci. **32**:37–43.
45. **Leist M, Single B, Castoldi AF, Kühnle S, Nicotera P.** 1997. Intracellular adenosine triphosphate (ATP) concentration: a switch in the decision between apoptosis and necrosis. J. Exp. Med. **185**:1481–1486.
46. **Scaffidi P, Misteli T, Bianchi ME.** 2002. Release of chromatin protein HMGB1 by necrotic cells triggers inflammation. Nature **418**:191–195.
47. **Feoktistova M, Geserick P, Kellert B, Dimitrova DP, Langlais C, Hupe M, Cain K, MacFarlane M, Häcker G, Leverkus M.** 2011. cIAPs block ripoptosome formation, a RIP1/caspase-8 containing intracellular cell death complex differentially regulated by cFLIP isoforms. Mol. Cell **43**: 449–463.
48. **Krysko DV, Vanden Berghe T, D'Herde K, Vandenabeele P.** 2008. Apoptosis and necrosis: detection, discrimination and phagocytosis. Methods **44**:205–221.
49. **Danthi P, Hansberger MW, Campbell JA, Forrest JC, Dermody TS.** 2006. JAM-A-independent, antibody-mediated uptake of reovirus into cells leads to apoptosis. J. Virol. **80**:1261–1270.
50. **He S, Wang L, Miao L, Wang T, Du F, Zhao L, Wang X.** 2009. Receptor interacting protein kinase-3 determines cellular necrotic response to TNF-alpha. Cell **137**:1100–1111.
51. **Clarke P, Meintzer SM, Gibson S, Widmann C, Garrington TP, Johnson GL, Tyler KL.** 2000. Reovirus-induced apoptosis is mediated by TRAIL. J. Virol. **74**:8135–8139.
52. **Tenev T, Bianchi K, Darding M, Broemer M, Langlais C, Wallberg F, Zachariou A, Lopez J, MacFarlane M, Cain K, Meier P.** 2011. The Ripoptosome, a signaling platform that assembles in response to genotoxic stress and loss of IAPs. Mol. Cell **43**:432–448.
53. **Upton JW, Kaiser WJ, Mocarski ES.** 2012. Dai/ZBP1/DLM-1 complexes with RIP3 to mediate virus-induced programmed necrosis that is targeted by murine cytomegalovirus vIRA. Cell Host Microbe **11**:290–297.
54. **Bertrand MJ, Vandenabeele P.** 2011. The Ripoptosome: death decision in the cytosol. Mol. Cell **43**:323–325.
55. **Marcato P, Shmulevitz M, Pan D, Stoltz D, Lee PW.** 2007. Ras transformation mediates reovirus oncolysis by enhancing virus uncoating, particle infectivity, and apoptosis-dependent release. Mol. Ther. **15**: 1522–1530.
56. **Wisniewski ML, Werner BG, Hom LG, Anguish LJ, Coffey CM, Parker JS.** 2011. Reovirus infection or ectopic expression of outer capsid protein micro1 induces apoptosis independently of the cellular proapoptotic proteins Bax and Bak. J. Virol. **85**:296–304.
57. **Coffey CM, Sheh A, Kim IS, Chandran K, Nibert ML, Parker JS.** 2006. Reovirus outer capsid protein micro1 induces apoptosis and associates with lipid droplets, endoplasmic reticulum, and mitochondria. J. Virol. **80**:8422–8438.
58. **Knowlton JJ, Dermody TS, Holm GH.** 2012. Apoptosis induced by mammalian reovirus is beta interferon (IFN) independent and enhanced by IFN regulatory factor 3- and NF-κB-dependent expression of noxa. J. Virol. **86**:1650–1660.
59. **Beckham JD, Tuttle KD, Tyler KL.** 2010. Caspase-3 activation is required for reovirus-induced encephalitis in vivo. J. Neurovirol. **16**:306–317.
60. **Barton ES, Youree BE, Ebert DH, Forrest JC, Connolly JL, Valyi-Nagy T, Washington K, Wetzel JD, Dermody TS.** 2003. Utilization of sialic acid as a coreceptor is required for reovirus-induced biliary disease. J. Clin. Invest. **111**:1823–1833.
61. **Papadimitriou JM.** 1968. The biliary tract in acute murine reovirus 3 infection. Light and electron microscopic study. Am. J. Pathol. **52**: 595–601.
62. **Derrien M, Hooper JW, Fields BN.** 2003. The M2 gene segment is involved in the capacity of reovirus type 3Abney to induce the oily fur syndrome in neonatal mice, a S1 gene segment-associated phenotype. Virology **305**:25–30.
63. **Wilson GA, Morrison LA, Fields BN.** 1994. Association of the reovirus S1

gene with serotype 3-induced biliary atresia in mice. J. Virol. **68**: 6458–6465.
64. **Sherry B, Schoen FJ, Wenske E, Fields BN.** 1989. Derivation and characterization of an efficiently myocarditic reovirus variant. J. Virol. **63**: 4840–4849.
65. **Brojatsch J, Naughton J, Rolls MM, Zingler K, Young JA.** 1996. CAR1, a TNFR-related protein, is a cellular receptor for cytopathic avian leukosis-sarcoma viruses and mediates apoptosis. Cell **87**:845–855.
66. **Hanon E, Keil G, van Drunen Littel-van den Hurk S, Griebel P, Vanderplasschen A, Rijsewijk FA, Babiuk L, Pastoret PP.** 1999. Bovine herpesvirus 1-induced apoptotic cell death: role of glycoprotein D. Virology **257**:191–197.
67. **Gosselin AS, Simonin Y, Guivel-Benhassine F, Rincheval V, Vayssière JL, Mignotte B, Colbère-Garapin F, Couderc T, Blondel B.** 2003. Poliovirus-induced apoptosis is reduced in cells expressing a mutant CD155 selected during persistent poliovirus infection in neuroblastoma cells. J. Virol. **77**:790–798.
68. **Liu Y, Pu Y, Zhang X.** 2006. Role of the mitochondrial signaling pathway in murine coronavirus-induced oligodendrocyte apoptosis. J. Virol. **80**: 395–403.
69. **Jan JT, Griffin DE.** 1999. Induction of apoptosis by *sindbis* virus occurs at cell entry and does not require viral replication. J. Virol. **73**:10296–10302.
70. **Chinchar VG, Bryan L, Wang J, Long S, Chinchar GD.** 2003. Induction of apoptosis in frog virus 3-infected cells. Virology **306**:303–312.
71. **Ramsey-Ewing A, Moss B.** 1998. Apoptosis induced by a postbinding step of vaccinia virus entry into Chinese hamster ovary cells. Virology **242**: 138–149.
72. **Labrada L, Bodelón G, Viñuela J, Benavente J.** 2002. Avian reoviruses cause apoptosis in cultured cells: viral uncoating, but not viral gene expression, is required for apoptosis induction. J. Virol. **76**:7932–7941.
73. **Mortola E, Noad R, Roy P.** 2004. Bluetongue virus outer capsid proteins are sufficient to trigger apoptosis in mammalian cells. J. Virol. **78**: 2875–2883.
74. **Chan FK, Shisler J, Bixby JG, Felices M, Zheng L, Appel M, Orenstein J, Moss B, Lenardo MJ.** 2003. A role for tumor necrosis factor receptor-2 and receptor-interacting protein in programmed necrosis and antiviral responses. J. Biol. Chem. **278**:51613–51621.
75. **Chu JJ, Ng ML.** 2003. The mechanism of cell death during west Nile virus infection is dependent on initial infectious dose. J. Gen. Virol. **84**: 3305–3314.
76. **Li M, Beg AA.** 2000. Induction of necrotic-like cell death by tumor necrosis factor alpha and caspase inhibitors: novel mechanism for killing virus-infected cells. J. Virol. **74**:7470–7477.
77. **Kobayashi T, Ooms LS, Ikizler M, Chappell JD, Dermody TS.** 2010. An improved reverse genetics system for mammalian orthoreoviruses. Virology **398**:194–200.
78. **Kobayashi T, Antar AA, Boehme KW, Danthi P, Eby EA, Guglielmi KM, Holm GH, Johnson EM, Maginnis MS, Naik S, Skelton WB, Wetzel JD, Wilson GJ, Chappell JD, Dermody TS.** 2007. A plasmid-based reverse genetics system for animal double-stranded RNA viruses. Cell Host Microbe **1**:147–157.
79. **Berard A, Coombs KM.** 2009. Mammalian reoviruses: propagation, quantification, and storage. Curr. Protoc. Microbiol. Chapter 15: Unit15C.11.
80. **Virgin HW, IV, Bassel-Duby R, Fields BN, Tyler KL.** 1988. Antibody protects against lethal infection with the neurally spreading reovirus type 3 (Dearing). J. Virol. **62**:4594–4604.
81. **Smith RE, Zweerink HJ, Joklik WK.** 1969. Polypeptide components of virions, top component and cores of reovirus type 3. Virology **39**: 791–810.
82. **Wetzel JD, Chappell JD, Fogo AB, Dermody TS.** 1997. Efficiency of viral entry determines the capacity of murine erythroleukemia cells to support persistent infections by mammalian reoviruses. J. Virol. **71**:299–306.
83. **Becker MM, Peters TR, Dermody TS.** 2003. Reovirus sigma NS and mu NS proteins form cytoplasmic inclusion structures in the absence of viral infection. J. Virol. **77**:5948–5963.